

# Frequency Tunable and Circular Polarization Switchable Antenna Using Dual Polarized Active Artificial Ground Structure

B. Liang<sup>1,2</sup>, B. Sanz-Izquierdo<sup>1</sup>, E. A. Parker<sup>1</sup>, J. C. Batchelor<sup>1</sup>, M. Bai<sup>2</sup>, J. Miao<sup>2</sup>

<sup>1</sup> School of Engineering and Digital Arts, The University of Kent, Canterbury, United Kingdom, [b.sanz@kent.ac.uk](mailto:b.sanz@kent.ac.uk)

<sup>2</sup> School of Electronic and Information Engineering, Beihang University, Beijing, China

**Abstract**—This paper presents a frequency and polarization reconfigurable circular polarized (CP) antenna using active artificial ground (AG) structure. The active AG structure offers independent and symmetrical tuning capability of the reflection phases for dual polarized incident waves. By combining the AG structure with a wideband coplanar waveguide fed monopole antenna, and tuning the capacitances of the varactor diodes on the AG structure, CP wave is dynamically realized at any desired frequency over a wide band in the 1.15-1.60GHz range. At each frequency, the CP state is switchable between left hand CP and right hand CP, by simply swapping the capacitances of varactors controlling the reflection phases of the two orthogonal polarized waves. The antenna covers the frequencies of all operational and in-preparation satellite navigation systems, including GPS, GLONASS, Beidou and Galileo.

**Index Terms**—CP antenna, frequency tunable, polarization switchable, active artificial ground, satellite navigation.

## I. INTRODUCTION

Satellite navigation systems (SNS) have been widely used in military, commercial and civil applications, regarded as one of the most successful products for wireless communications. Based on the capability of identifying user locations, SNS offer position-related services. As the most well-known satellite navigation system, Global Positioning System (GPS) is maintained by the United States, capable of providing real-time and all-weather global navigation services for the areas of land, sea and air. For the sake of national securities, some other navigation systems are also in use or under preparation, such as GLONASS of Russia, Galileo of European Union, and Beidou of China.

Most SNS employ circular polarized (CP) antennas to transmit signals, due to their advantages of alleviating multipath interferences or fading, insensitivity to Faraday rotation effect, and no strict requirement of antenna orientations [1]. In order to cover frequency bands of various SNS with one antenna, wideband or multiband CP antennas for SNS have drawn increasing interests [2-4]. However, if one or more of these SNS bands were to be filtered at a certain time, passive antennas would not be suitable due to their fixed characteristics and absence of frequency selection. Alternatively, frequency reconfigurable antennas can provide not only the wideband feature to apply to any SNS, but also the flexibility of switching among frequency bands of different systems.

CP antennas can be realized through many manners, among which artificial ground (AG) structures have been employed as promising candidates, owing to the advantages of low profile and avoidance of using impedance matching networks [5, 6]. AG structures are electromagnetic band gap (EBG) structures without vias, hereby losing the ability of surface wave suppression but retaining the in-phase reflection behavior of EBG structures. By using the characteristics of the frequency-dependent reflection phases, AG structures can generate CP waves from linear polarized (LP) waves [7]. The designs of [6] and [7] exhibited dual and single narrow axial ratio (AR) bandwidths ( $AR \leq 3\text{dB}$ ) respectively, while the design of [5] offered an AR bandwidth of 20.4%. Since the frequency band covering all SNS is at least 1.16-1.60GHz [8], i.e. the fractal bandwidth of 32%, none of the aforementioned design using AG structures is adequate. As an alternative, AG structures can bring notable improvement in the bandwidth of the reflection phase, due to the tunable capacitance of active components [9-14]. Therefore, by incorporating active AG structures the operating frequency of CP waves can be tuned within a fairly wide range.

In this paper, we present a frequency tunable CP antenna, using an active AG structure. The active AG structure exhibits dual-polarized tunable reflection phases versus frequency, and tunings for orthogonal polarized incident plane waves are independent and symmetrical. A coplanar waveguide (CPW) fed monopole is used as the radiating antenna, in order to provide good input matching over a wide band. Simulation study were implemented by using CST Microwave Studio, and results suggest that CP waves can be realized between 1.15GHz-1.60GHz through tuning the capacitances of varactor diodes, capable of covering frequencies of any SNS. Owing to the symmetry of the configuration, agile polarization switching between right hand CP (RHCP) and left hand CP (LHCP) is also obtained.

## II. DUAL POLARIZED ACTIVE AG STRUCTURE

The schematic diagram of the active AG structure is presented in Fig. 1. The periodic square-patch layer (PSPL) and the ground plane are spaced by an air layer, with the height of  $h$ . A polyester substrate ( $\epsilon_r = 3$ ) of 0.05mm thickness with metal cladding on its two sides is used to form the PSPL, and the square patches are printed on both sides. As seen in Fig.

1(d), the upper and lower layers are overlapped in x-y plane. On the upper layer, varactor diodes are located between adjacent patches along y-direction, while the DC continuity of each row is provided by surface mount resistors, as well as the voltages simultaneously supplied from left and right ends. The arrangement of varactor diodes and biasing circuits on the lower layer is in the same way but along the perpendicular direction. Owing to the symmetry of the biasing circuit in each row or column, the voltage drop caused by the very small current flowing across the diodes can be neglected, especially when the array size is not large [15-17].

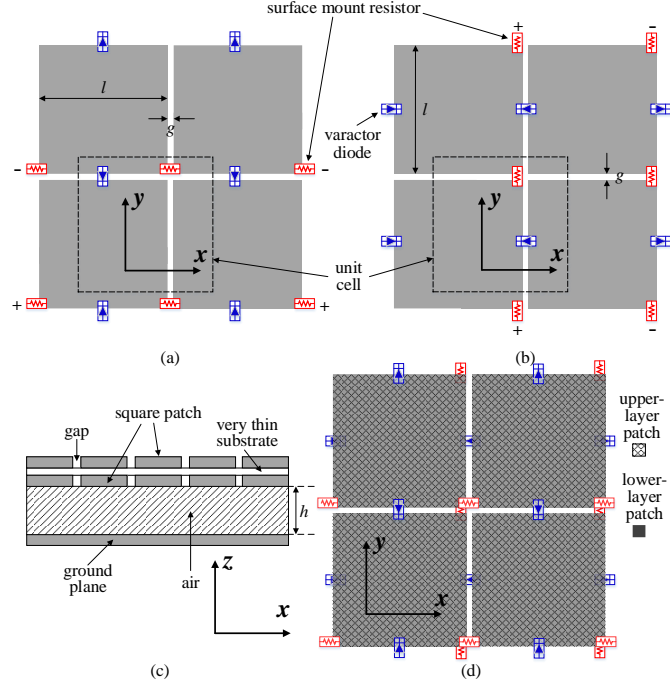


Fig. 1. Unit cells of the dual polarized active AG structure with varactors and resistors. (a) upper layer (b) lower layer (c) magnified cross-sectional view (d) alignment of the upper and lower layers

The incorporated varactor diodes were BB857, modeled as a series RLC circuit in simulation. According to the datasheet, the series resistance and inductance are  $1.5\Omega$  and  $0.6\text{nH}$  respectively, and the variable capacitance can be tuned from  $0.55\text{pF}$  to  $6.6\text{pF}$ . In the following, the uniform capacitances of varactors on the upper and lower layers are defined as  $C_1$  and  $C_2$  respectively.

In order to demonstrate the polarization-independent and symmetrical tuning ability,  $C_1$  and  $C_2$  were varied from  $0.55\text{pF}$  to  $3.55\text{pF}$  in simulation. Other parameters are set as follows:  $l=21\text{mm}$ ,  $g=1\text{mm}$ ,  $h=5\text{mm}$ . As shown in Fig. 2(a), when  $C_1$  is fixed to  $0.55\text{pF}$  while  $C_2$  is decreased, the phase curve of the x-polarization shift towards higher frequencies, while the phases of the y-polarization remains stable. Hence, the independent tuning capability for dual polarizations is verified. It is also indicated that the reflection phases for the x- and y-polarized waves agree very well with each other when both capacitances are  $0.55\text{pF}$ , demonstrating the tuning symmetry for the dual polarizations. Similarly, the phase stability of tuning for the orthogonal polarization in lower frequencies is illustrated in Fig. 2(b), as well as the polarization symmetry.

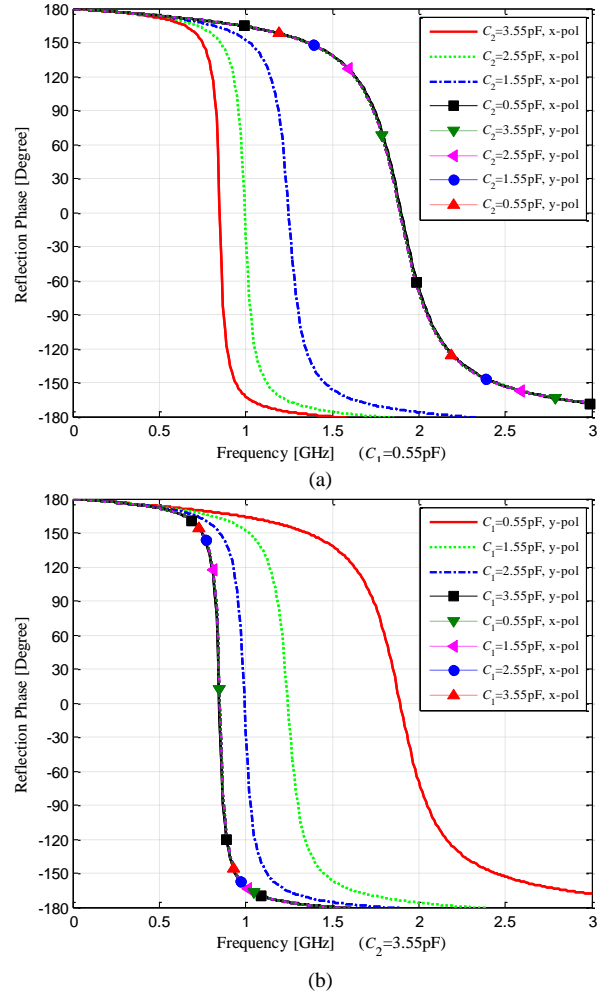


Fig. 2. Tunable reflection phases for dual polarizations (a)  $C_1$  is fixed,  $C_2$  is varied (b)  $C_2$  is fixed,  $C_1$  is varied

### III. WIDEBAND RECONFIGURABLE CP ANTENNA USING ACTIVE AG STRUCTURE

#### A. Configuration

The schematic diagram of the antenna is shown in Fig. 3, in which the resistors are hidden for clarity. The AG structure consists of  $6\times 6$  unit cells, and a CPW monopole antenna rotated by  $45^\circ$  with respect to the EBG lattice is placed above the upper patch layer, with a distance of  $h'$ .

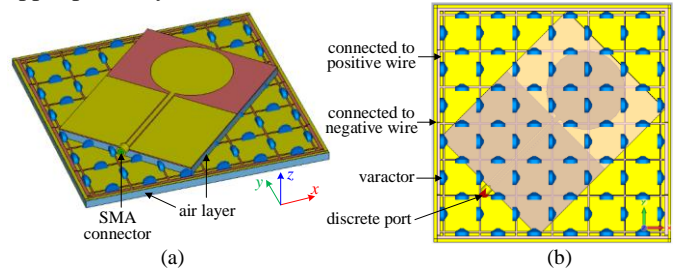


Fig. 3. Schematic diagram of the antenna (a) perspective view (b) top view

Similar to the dipole used in [7], the CPW monopole radiates omnidirectional LP waves in the plane of  $\phi=135^\circ$  in Fig. 3, but offering a broadband input matching. The dimensions

and reflection coefficient of the monopole are presented in Fig. 4. The substrate of the monopole is Rogers 5870, with  $\epsilon_r$  of 2.33 and the thickness of 0.787mm. According to the composition principle of the directly radiated wave and the reflected wave described in [7], the LP waves can be converted to CP waves over a wide band. The theoretical condition to generate CP waves is the reflection phase for one-polarized wave equals to  $90^\circ$ , while the phase for the other polarization is  $-90^\circ$ . However, the distance and multiple reflections between the antenna and the AG surface were ignored in the derivation process, as well as the infinity of the AG structure. Therefore, in order to obtain accurate prediction of the antenna performances, the entire structure including the varactor diodes should be modeled in CST, rather than simply referring to the values of  $C_1$  and  $C_2$  obtained in the unit cell simulation.

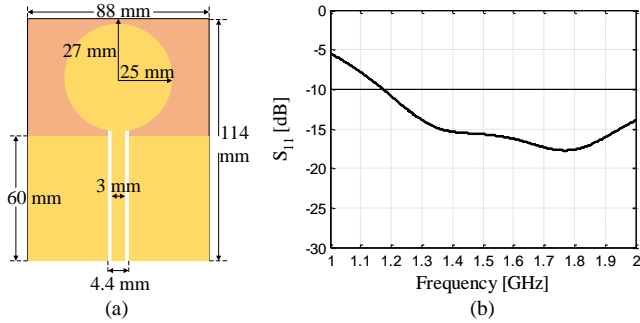


Fig. 4. The CPW monopole antenna (a) top view (b) reflection coefficient

### B. Frequency Tunable Capability

According to the datasheet of BB857 varactor diodes, the lowest tunable capacitance is 0.55pF, corresponding to the highest frequency acquiring high-quality AR. Hence by fixing  $C_1 = 0.55\text{pF}$ ,  $h = h' = 5\text{mm}$ , and optimizing  $C_2$  and the side length  $l$  of the square patch of the AG structure, a fairly low broadside AR was obtained at the target highest operating frequency 1.60GHz. The optimal parameters are as follows:  $C_2 = 1.25\text{pF}$ , and  $l = 22\text{mm}$ .

As aforementioned, the reflection phase curves for dual polarizations can be tuned continuously towards lower frequencies, as the capacitances increase. Therefore, by tuning  $C_1$  and  $C_2$  to a certain pair of values, any desired frequencies over a wide band are certain to achieve low-level ARs. To demonstrate this tuning capability, the AR curves are tuned to reach a valley of low value at four sampling frequencies from 1.15GHz to 1.60GHz respectively. Fig. 5 presents the simulated ARs and reflection coefficients. It can be seen that not only satisfactory ARs are reached at the four frequencies, but also  $S_{11}$  less than -10dB are obtained respectively, owing to the wideband matching characteristics of the radiating monopole antenna. The radiation patterns at each frequency are presented in Fig. 6, in which low cross-polarizations within a wide range of angles can be observed. In order to clearly show the varying tendency of  $C_1$  and  $C_2$  in the tuning process, their values to realize CP characteristics at the four frequencies are plotted in Fig. 7. It is found that both  $C_1$  and  $C_2$  are in approximately linear variation over the band between 1.15-1.60GHz, which can be a helpful guide to efficiently tune the AR frequency onto any other frequencies over the frequency range. The di-

rectivity and gain at each frequency are also presented in Fig. 7, and the gains are found to drop dramatically in lower frequencies. This is due to the low quality factor of the varactor diodes when series capacitance is high.

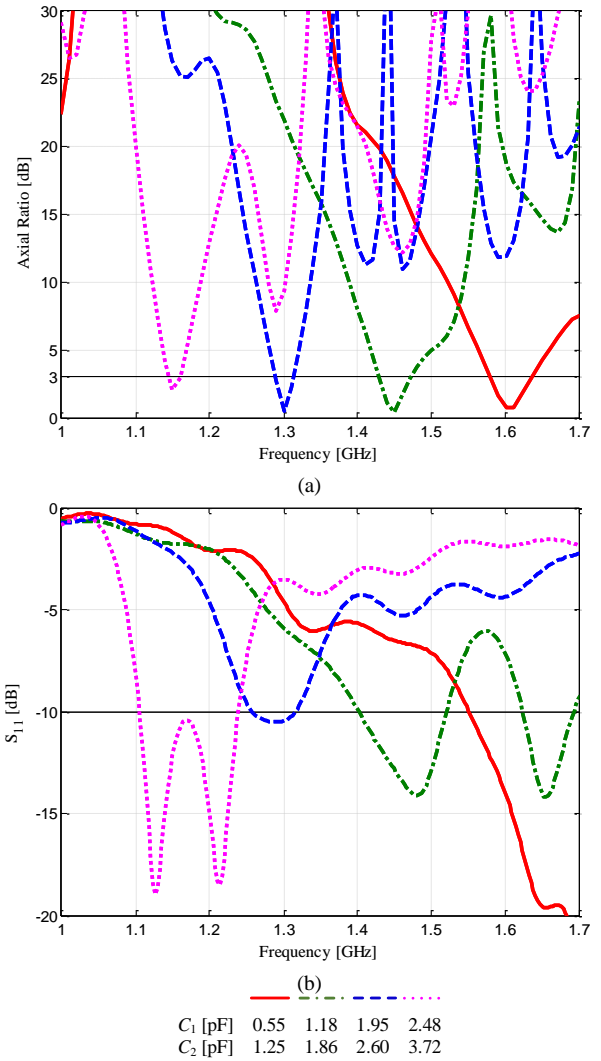


Fig. 5. Illustration of tuning capability (a) AR (b) reflection coefficients

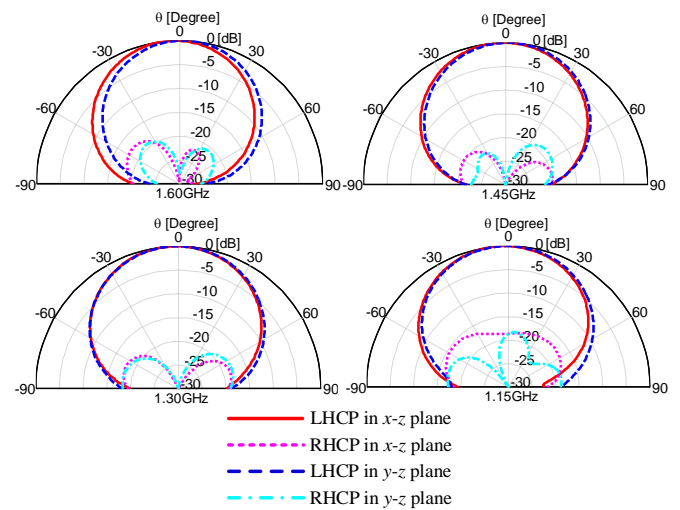


Fig. 6. Radiation patterns at four sampling frequencies

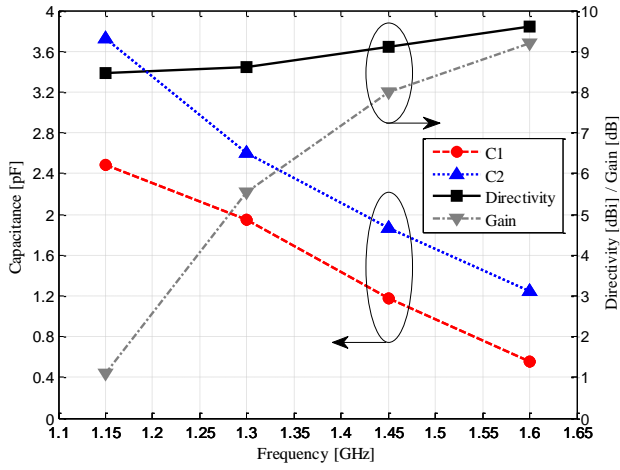


Fig. 7. Capacitances, directivity and gain at each frequency

### C. Polarization Switchable Capability

In the previous sub-section,  $C_1$  remained less than  $C_2$ , so LHCP was the co-polarization at all cases. Considering the symmetry of the reflection phases for dual polarizations and the antenna configuration, LHCP can be changed into RHCP by simply swapping  $C_1$  and  $C_2$ . To conserve space, the case of 1.45GHz is taken as an example.

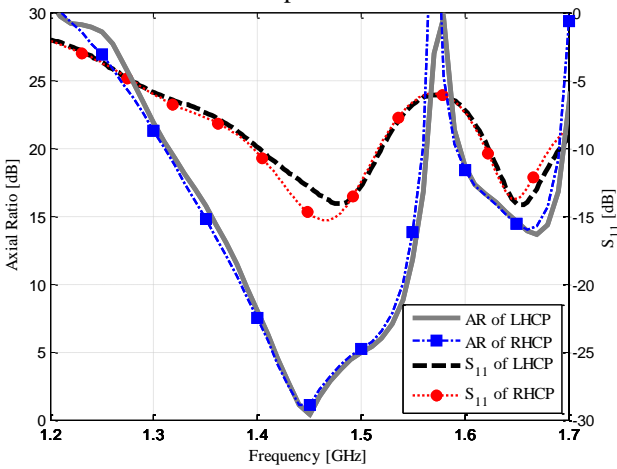


Fig. 8. Switchable capability in terms of AR and  $S_{11}$  versus frequency

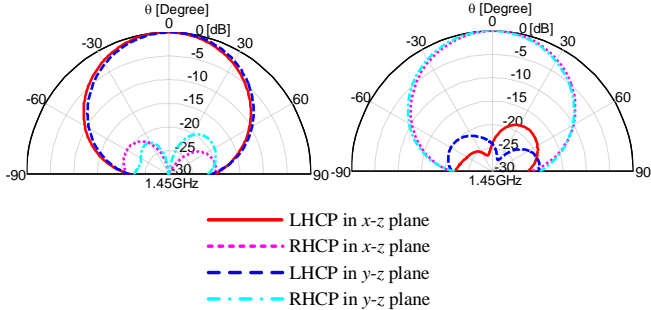


Fig. 9. Switchable capability in terms of radiation patterns

According to Fig. 5(a), LHCP was realized at 1.45GHz when  $C_1=1.18\text{pF}$  and  $C_2=1.86\text{pF}$ . Fig. 8 presents the AR and  $S_{11}$  curves before and after swapping  $C_1$  and  $C_2$ , showing good agreements between the LHCP and RHCP cases. The radiation patterns at 1.45GHz of the two cases are shown in Fig. 9. In

the left figure the co-polarization is LHCP, while in the right figure it is RHCP. Hence, the capability of the switchable CP polarization is clearly demonstrated.

## IV. PRELIMINARY EXPERIMENTAL RESULT

A structure of similar characteristics to the one described in section III was fabricated as shown in Fig.10, and its radiating characteristics were measured in an anechoic chamber. In order to demonstrate the frequency reconfigurability, five curves with well-tuned AR values at five different frequencies are presented in Fig. 11. The five curves correspond to the cases from A to E listed in Table I, and voltage supplies of each case in measurement are also provided. In addition, the measured  $S_{11}$  of the antenna in each case was lower than -10dB, exhibiting satisfactory matching performance.

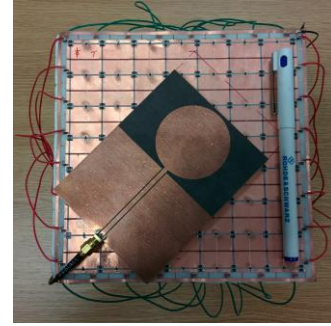


Fig. 10. Fabricated prototype

TABLE I  
TUNING CHARACTERISTICS OF DIFFERENT CASES

	$U_1$ (Volt)	$U_2$ (Volt)	Frequency (GHz)	Polarization
Case A	29.50	10.68	1.52	LHCP
Case B	13.23	7.39	1.38	LHCP
Case C	9.62	6.18	1.30	LHCP
Case C*	6.18	9.62	1.30	RHCP
Case D	6.95	4.91	1.20	LHCP
Case E	5.73	3.53	1.10	LHCP

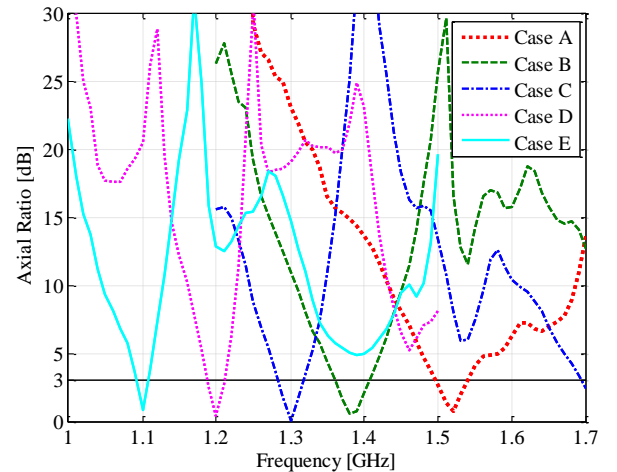


Fig. 11. Measured ARs versus frequency for the configuration in Fig.10.

The switching function between LHCP and RHCP is illustrated in Fig. 12. Case C\* was implemented in the measurement, by repeating Case C but swapping  $U_1$  and  $U_2$ . The AR

and  $S_{11}$  curves versus frequency are presented. It can be seen that good agreement of curves between the original case and the star case is obtained, especially near the CP operating frequencies. The radiation patterns at 1.30GHz of Case C and C\* are shown in Fig. 13(a) and (b) respectively. It is verified that the co-polarization can be switched from LHCP to RHCP, by simply swapping  $U_1$  and  $U_2$ .

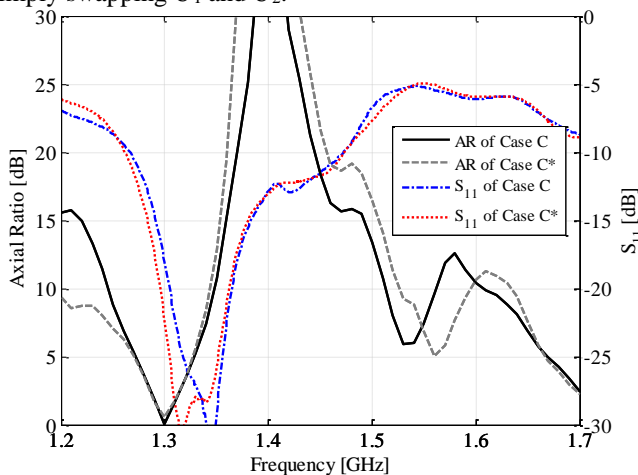


Fig. 12. Measured AR and  $S_{11}$  vs frequency for the configuration in Fig. 10

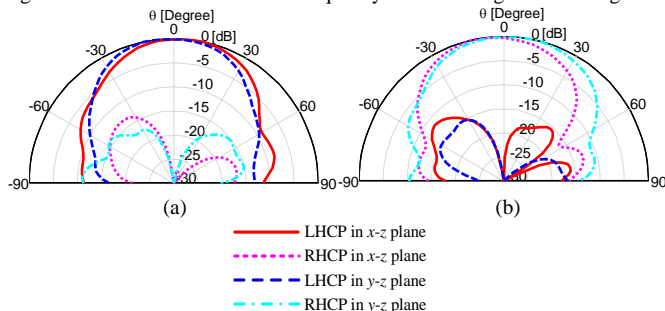


Fig. 13. Measured radiation patterns for the configuration in Fig. 10.

## V. CONCLUSION AND DISCUSSION

A reconfigurable antenna using CPW fed monopole and active AG structure has been presented. The active AG structure consists of a 0.05mm-thick polyester substrate with periodic square patches cladding on its two sides, and the underneath ground plane spaced by an air layer. Varactor diodes are employed to connect adjacent patches on each side of the substrate along x- and y- directions respectively, and surface mount resistors of 10k $\Omega$  are used as the biasing circuit. The AG structure exhibits tunable capability of the reflection phases for dual polarizations, and tunings for the x- and the y- polarizations are symmetrical and independent. By tuning the varactor capacitances in the two directions together, high-quality ARs can be obtained over a wide band covering the frequencies of all satellite navigation systems. As a demonstration, CP characteristics at four equally spaced frequencies from 1.15GHz to 1.60GHz are presented, and input reflection coefficients of less than -10dB are also obtained at each frequency.

By swapping the capacitances of the varactors on the two patch layers, the LHCP is converted to right hand circular polarization RHCP straightforwardly. The antenna efficiency is found to be significantly reduced in lower frequencies, due to the series resistance and the high capacitance of the varactor diodes. The frequency and polarization reconfigurabilities are also verified in the measurement.

## REFERENCES

- [1] S. Gao, Q. Luo, and F. Zhu, *Circularly polarized antennas*: John Wiley & Sons, 2013.
- [2] G. Massie, M. Caillet, M. Clénet, and Y. M. Antar, "A new wideband circularly polarized hybrid dielectric resonator antenna," *Antennas and Wireless Propagation Letters, IEEE*, vol. 9, pp. 347-350, 2010.
- [3] L. Wang, Y. X. Guo, and W. Sheng, "Tri-band circularly polarized annular slot antenna for GPS and CNSS applications," *Journal of Electromagnetic Waves and Applications*, vol. 26, pp. 1820-1827, 2012.
- [4] S.-H. Chang and W.-J. Liao, "A novel dual band circularly polarized GNSS antenna for handheld devices," *Antennas and Propagation, IEEE Transactions on*, vol. 61, pp. 555-562, 2013.
- [5] T. Nakamura and T. Fukusako, "Broadband design of circularly polarized microstrip patch antenna using artificial ground structure with rectangular unit cells," *Antennas and Propagation, IEEE Transactions on*, vol. 59, pp. 2103-2110, 2011.
- [6] H. Yi and S. W. Qu, "A Novel Dual-Band Circularly Polarized Antenna Based on Electromagnetic Band-Gap Structure," *IEEE Antennas Wireless Propag. Lett.*, vol. 12, pp. 1149-1152, 2013.
- [7] F. Yang and Y. Rahmat-Samii, "A low profile single dipole antenna radiating circularly polarized waves," *Antennas and Propagation, IEEE Transactions on*, vol. 53, pp. 3083-3086, 2005.
- [8] [http://en.wikipedia.org/wiki/Satellite\\_navigation](http://en.wikipedia.org/wiki/Satellite_navigation).
- [9] L. Boccia, F. Venneri, G. Amendola, and G. Di Massa, "Application of varactor diodes for reflectarray phase control," in *Antennas and Propagation Society International Symposium, 2002. IEEE*, 2002, p. 132.
- [10] D. Sievenpiper and J. Schaffner, "Beam steering microwave reflector based on electrically tunable impedance surface," *Electronics Letters*, vol. 38, pp. 1237-1238, 2002.
- [11] D. F. Sievenpiper, J. H. Schaffner, H. J. Song, R. Y. Loo, and G. Tangonan, "Two-dimensional beam steering using an electrically tunable impedance surface," *Antennas and Propagation, IEEE Transactions on*, vol. 51, pp. 2713-2722, 2003.
- [12] C. Mias and J. H. Yap, "A varactor-tunable high impedance surface with a resistive-lumped-element biasing grid," *Antennas and Propagation, IEEE Transactions on*, vol. 55, pp. 1955-1962, 2007.
- [13] H. J. Lee, R. Langley, and K. Ford, "Tunable active EBG," in *Antennas and Propagation, 2007. EuCAP 2007. The Second European Conference on*, 2007, pp. 1-4.
- [14] H. Lee, K. Ford, and R. Langley, "Dual band tunable EBG," *Electronics Letters*, vol. 44, pp. 392-394, 2008.
- [15] B. Sanz-Izquierdo, E. A. Parker, J. B. Robertson, and J. C. Batchelor, "Tuning patch-form FSS," *Electronics Letters*, vol. 46, pp. 329-330, 2010.
- [16] C. Mias, "Varactor-tunable frequency selective surface with resistive-lumped-element biasing grids," *Microwave and Wireless Components Letters, IEEE*, vol. 15, pp. 570-572, 2005.
- [17] B. Sanz-Izquierdo and E. A. Parker, "Dual Polarized Reconfigurable Frequency Selective Surfaces," *Antennas and Propagation, IEEE Transactions on*, vol. 62, pp. 764 - 771, 2014.